Fizika Nizkikh Temperatur, 2008, v. 34, No. 3, p. 219–224

Ionic cluster effect in suppression on superconductivity in Ni- and Co-doped YBCO systems

Aihua Wang, Xiaoxia Wang, Yigang Cao, Xinli Li, Yongyong Wang, Liming Gao, Heqiang Lu, Jie Zhang, and Pinglin Li

School of Physics and Engineering, Zhengzhou University, Zhengzhou 450001, P. R. China
E-mail: lipinglin@zzu.edu.cn

Received September 17, 2007

We adopted the x-ray diffraction, oxygen contents, positron annihilation technology as well as simulation methods to investigate systemically $YBa_2Cu_{3-x}(Ni,Co)_xO_{7-\delta}$ (x = 0–0.5). The simulated results show that ions distribute in dispersive form in little doped concentration. As doped concentration increases, ions combine into clusters in the crystal lattice. The calculated results and oxygen contents, together with the impure phases and the local electron density n_e, show the ionic cluster effect, which not only causes the local electron density to reach the saturation, but also suppress the superconductivity significantly.

PACS: 47.54.De Experimental aspects;
47.54.Bd Theoretical aspects;
68.65.–k Low-dimensional, mesoscopic, and nanoscale systems: structure and nonelectronic properties.

Keywords: YBCO, ionic cluster effect, simulations, positron annihilation.

1. Introduction

There is continuing interest in the YBCO superconductor due to the typical CuO_2 plane and Cu–O chain structure [1–3], which have been studying prevalently so far [4,5]. In order to recognize the role of CuO_2 planes and Cu–O chains in cuprates, elemental substitution is an effective means [6–8]. Typical elements, including Fe, Co, Ni, Al, Zn, etc, can all be regarded as substitute for Cu sites. Among them, magnetic Ni and Co ions indicate some special significations in our research for the following reasons: firstly, although both of them are magnetic ions, they depress differently the T_c at the same doped concentration; secondly, Co ions can substitute for the Cu(1) sites in Cu–O chains, while Ni ions are rather complex on the substitution position. Again, as doped concentration increases, oxygen contents show different variations in the Ni- and Co-doped samples [9,10]. All of these factors indicate that some vital problems of Ni and Co doping should be researched further.

Though it is commonly known that all elements in substitution for Cu sites mostly enter CuO_2 planes or Cu–O chains [11], but how they enter is unclear. In what follows, we introduce the simulation method [12] to calculate the total defect energy of different clusters, and average binding energy per ion. The results indicate that the ions on CuO_2 planes tend to form the cluster of 7 ions as double square, and the ions in Cu–O chains tend to form the cluster of 6 ions as hexamer. When occupying the Cu(2) sites on CuO_2 planes, the clustering ions will directly influence the carriers' pairing and transportation, so the superconductivity is suppressed significantly [13]. In summary, except the ions doped sites, the ionic cluster effect also suppresses the superconductivity significantly.

2. Experiments and simulations

Samples of $YBa_2Cu_{3-x}M_xO_y$ (M = Ni, Co; x = 0–0.5) were prepared by solid-state reactions with the analytical purity Y_2O_3, $BaCO_3$, CuO, Co_2O_3, and Ni_2O_3. The raw materials were thoroughly pulverized into powder, which was put in the crucible and calcined first at 930 °C for 18 hours in air, and then the precursor sample was naturally cooled to room temperature in the furnace. Subsequently, the reground precursor was pressed into small wafers and sintered at 940 °C for 24 hours in above cooling process. Due to the sensitivity of positron annihilation technology (PAT) experiments, all samples were sintered under the

same conditions to reduce the dispersion of the experimental results. The superconducting transition temperature T_c was measured by the standard dc four-probe method with a voltage resolution of 10^{-7} V (HP3457A). The structure of the samples was analyzed by powder x-ray diffraction (XRD) (Cu-K_α) , using D/max-BX-ray diffractometer. The positron lifetime spectra were measured at constant temperature (283±1) K by the ORTEC-100U fast-fast coincidence lifetime spectrometer. Two pieces of identical samples (∅13×3 mm) were sandwiched together with a 10 μC ^{22}Na positron source deposited on a thin Mylar foil (of 1.2 mg/cm^2 thickness). We applied Pilot-U plastic flicker sensor, which was measured by ^{60}Co and showed the excellent time distinguishing rate over 220 ps. Each spectrum contains more than $1\cdot10^6$ counts to guarantee sufficient statistical precision. After subtracting background and source contributions, the lifetime spectra were analyzed in two-lifetime components by POSITRON-FIT-EXTENDED program with the best fit (χ^2 = 1.0–1.1). The positron lifetime spectra of all samples were measured at the identical environment and the results were repeatable.

In order to identify the distribution patterns of doped ions in clusters, we calculate the total defect energy of different clusters and average binding energy per ion. The calculations are based on the crystal lattice simulations on energy minimization principle and formulated within the framework of Born model, in which the effective pairwise potentials represent the interatomic forces in the following form [12]:

$$\Phi_{ij} = \frac{Z_i Z_j e^2}{4\pi\varepsilon_0 r_{ij}} + A_{ij} \exp\left(-\frac{r_{ij}}{\rho_{ij}}\right) - \frac{C_{ij}}{r_{ij}^6}, \qquad (1)$$

where Φ_{ij} is the effective potentials between ions i and j; Z_i and Z_j are ion valences; r_{ij} is the distance between ions i and j; A_{ij} , C_{ij} and ρ_{ij} are the relative character constants. The first term denotes the long-range Coulomb interaction, and the remaining terms represent the short-range interaction and the shielded revision. Because the charge equilibrium determines the ion coordination characteristics, the clusters should be neutral in electricity. For example, in 4 ions cluster on CuO_2 planes, Ni^{2+} ions are the substitute for $Cu^{2.25+}$ and holes exist on oxygen ions [14,15]. These two factors induce together the decrease of electron in the cluster; as a result, the oxygen ions have to decrease on CuO_2 planes due to the charge equilibrium. Namely, every four Ni^{2+} may exclude an oxygen ion from CuO_2 planes, which can be described as $4Ni^{2+} \rightarrow 4Cu^{2.25+} - O^{2-}$. However, one Ni^{2+} ions alone can't exclude an oxygen ion from CuO_2 planes. Hence, the binding energy of $4Ni^{2+}$ cluster is

$$E_{\text{bind}} = E_{b1}(4Ni^{2+} \rightarrow 4Cu^{2.25+} - O^{2-}) - 4E_{b2}(Ni^{2+} \rightarrow Cu^{2.25+}) + E_{b3}(O^{2-}), \qquad (2)$$

where E_{b1}, E_{b2} and E_{b3} are all represented by $E = \Sigma\Phi_{ij}$; E_{b1} is the total binding energy of a cluster, E_{b2} is the binding energy of a Ni^{2+} substitution for a $Cu^{2.25+}$ ion, and E_{b3} is the binding energy of lost O^{2-} ion. While every doped ion has the average binding energy $E_{\text{mean}} = E_{\text{bind}}/4$, where 4 is the number of doped ions in a cluster. Other clusters may be described and calculated likewise. The results of Ni^{2+} and Ni^{3+}doping are summarized in Table 1 and Table 2, respectively, while the results of Co doping are listed in Table 3.

Table 1. The total defect energy of Ni^{2+}–oxygen vacancies and the average binding of per ion on CuO_2 planes. Here the negative value indicates the binding energy. E_{b1} (eV) is total defect binding energy in a cluster, and E_{mean} (eV/ion) is the average binding energy for per doped ion.

Cluster structure	E_{b1}, eV	E_{mean} , eV/ion
Dimmer $\{2Ni^{2+} \rightarrow 2Cu^{2.25+} - O^{2-}\}$	–30.37	–1.60
Tetramer $\{4Ni^{2+} \rightarrow 4Cu^{2.25+} - O^{2-}\}$ linear	–59.76	–1.25
Tetramer $\{4Ni^{2+} \rightarrow 4Cu^{2.25+} - O^{2-}\}$ square	–60.49	–1.59
Tetramer $\{4Ni^{2+} \rightarrow 4Cu^{2.25+} - O^{2-}\}$ zigzag	–59.25	–1.23
Hexamer $\{6Ni^{2+} \rightarrow 6Cu^{2.25+} - 2O^{2-}\}$	–95.43	–1.61
Hexamer $\{6Ni^{2+} \rightarrow 6Cu^{2.25+} - O^{2-}\}$	–104.98	–1.73
Double square $\{7Ni^{2+} \rightarrow 7Cu^{2.25+} - 2O^{2-}\}$	–118.72	–1.77

Table 2. The total defect energy of Ni^{3+} –interstitial oxygen and the average binding of per ion in Cu–O chains. Others are the same meaning as Table 1.

Cluster structure	E_{b1}, eV	E_{mean}, eV/ion
Dimmer $\{2Ni^{3+} \rightarrow 2Cu^{2+} + O^{2-}\}$	–50.98	–2.77
Tetramer $\{4\ Ni^{3+} \rightarrow 4Cu^{2+} + 2O^{2-}\}$ linear	–100.34	–2.35
Tetramer $\{4Ni^{3+} \rightarrow 4Cu^{2+} + 2O^{2-}\}$ square	–101.87	–2.74
Tetramer $\{4\ Ni^{3+} \rightarrow 4Cu^{2+} + 2O^{2-}\}$ zigzag	–99.19	–2.02
Hexamer $\{6Ni^{3+} \rightarrow 6Cu^{2+} + 4O^{2-}\}$	–167.66	–2. 83
Double square $\{7Ni^{3+} \rightarrow 7Cu^{2+} + 4O^{2-}\}$	–188.13	–2. 79

Table 3. The total defect energy of Co^{3+} –interstitial oxygen and the average binding of per ion in Cu–O chains. Others are the same meaning as Table 1.

Cluster structure	E_{b1}, eV	E_{mean}, eV/ion
Dimmer $\{2Co^{3+} \rightarrow 2Cu^{2+} + O^{2-}\}$	–56.27	–2.80
Tetramer$\{4Co^{3+} \rightarrow 4Cu^{2+} + 2O^{2-}\}$ linear	–111.53	–2.44
Tetramer$\{4Co^{3+} \rightarrow 4Cu^{2+} + 2O^{2-}\}$ square	–112.37	–2.82
Tetramer $\{4Co^{3+} \rightarrow 4Cu^{2+} + 2O^{2-}\}$ zigzag	–110.18	–2.05
Hexamer $\{6Co^{3+} \rightarrow 6Cu^{2+} + 4O^{2-}\}$	–188.72	–3.03
Double square $\{7Co^{3+} \rightarrow 7Cu^{2+} + 4O^{2-}\}$	–208.98	–2.91

3. Experimental results and discussions

3.1. The structure and superconductivity in doped samples

The XRD results indicate that undoped $YBa_2Cu_3O_{7-\delta}$ has an excellent single-phased structure. With doped concentration increasing, a few impure phases appear at $x = 0.20$ for Ni doping, and at $x = 0.25$ for Co. Figure 1 shows lattice parameter a and b variation with Ni and Co concentration x. For Ni doping, a and b approach obviously before $x = 0.20$, but an O–T transition does not occur until $x = 0.5$. Other experimental results indicate the same characteristics [16]. While for Co-doping, the O–T transition appears near $x = 0.12$. In fact, many experiments and analyses reveal that the O–T transition originates from the increase of oxygen content in Cu–O chains [17]. That is, every two +3 valence ions will make an extra oxygen ion enter a axis [13], then the O–T transition occurs. As indicated by above analysis, Co ions mainly enter Cu(1) sites. However, Ni ions distribution present much more complicated pattern, since a and b variation imply that Ni ions do not only occupy Cu(1) or Cu(2) sites, but also may shift sites with x increasing .

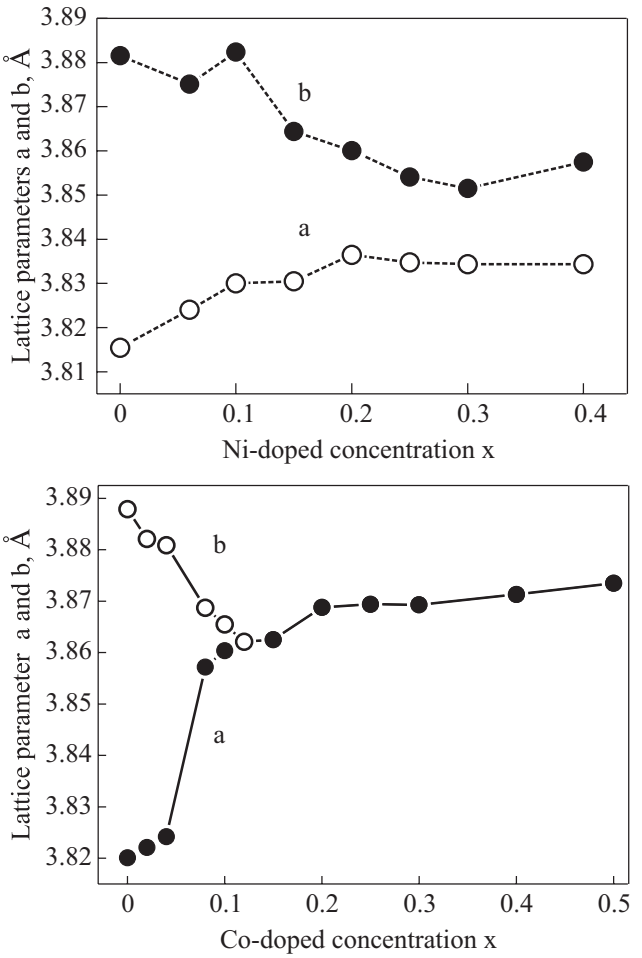

Fig. 1. Lattice parameter a and b variation with Ni- and Co-doped concentration x in $YBa_2Cu_{3-x}(Ni,Co)_xO_{7-\delta}$.

Figure 2 shows that the T_c variation depends on Ni and Co concentration x. For undoped sample, the T_c is 91.5 K. Only little Ni doping depresses the T_c significantly, namely, the T_c falls quickly to about 60 K at $x = 0.05$, then the T_c falls gradually slowly. This characteristic reveals that Ni ions on CuO_2 planes decrease with x increasing. For Co-doped samples, the T_c decreases in stair with x increasing. With regard to the function of Cu(1) and Cu(2) sites, the general standpoint is that free carriers distribute on CuO_2 planes, and play a vital role in superconductivity. If the doped ions enter CuO_2 planes, even little doping depresses T_c significantly. In general, +2 valence ions tend to enter CuO_2 planes; while +3 valence ions tend to enter Cu–O chains. Acting as carrier reservoirs, Cu–O chains just play an indirect role in superconductivity [18,19]. As a result, little doping depresses T_c weakly. As x increases, the T_c is depressed gradually powerfully. The experimental evidences suggest that the doped sites, especially CuO_2 planes, are most important factors of influ-

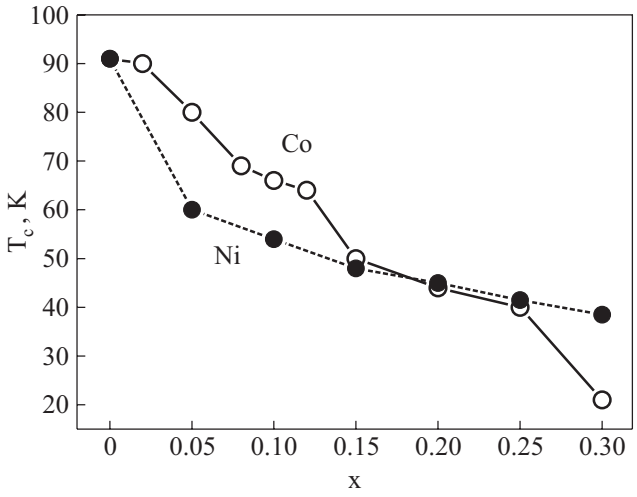

Fig. 2. Superconducting transition temperature T_c variation with Ni and Co concentration x in $YBa_2Cu_{3-x}(Ni,Co)_xO_{7-\delta}$.

ence on the superconductivity. In addition, the cross of two T_c curves in Fig. 2 implies another significant factor, the cluster effect.

3.2. Ionic cluster effect from oxygen contents and impure phases

As shown in the tables, those doped ions tend to form clusters. According to the solid theory, the larger the average binding energy E_{mean} is the more stable the cluster combines. Consequently, the ions with the largest average binding energy should form the cluster in the largest probability. In particular, +3 valence ions tend to form hexamer clusters of 6 ions in Cu–O chains. While for +2 valence ions, double-square clusters of 7 ions have the largest probability on CuO_2 planes. (Please, see the above two cluster structure in Fig. 4 of Ref. 13.) In general, the individual doped ions can not extrude or capture oxygen ions due to charge equilibrium, while the clustered ions can enable the oxygen content to change. The experimental results demonstrate that the oxygen content rises with x increasing in Co-doped samples, but it is basically invariable in Ni-doped samples on the whole [16], as shown in Fig. 3. According to the largest probability from the tables, every 7 Ni^{2+} extrude 2 oxygen ions from CuO_2 planes, while every 6 Ni^{3+} capture 4 oxygen ions in Cu–O chains. In order to keep the invariable characteristics, the ratio of Ni^{3+} to Ni^{2+} should be $(6/4)/(7/2) \approx {}^{1}/_{2.33}$, namely, the Ni^{2+} amount is 2.33 times of the Ni^{3+}.

As mentioned above, the impure peaks appear at $x = 0.20$, which means that all doped Ni ions enter the crystal lattice before $x = 0.20$. Consequently, the Ni ions in Cu(1) sites is actually only $x_1 = 0.20 \times 1/(2.33 + 1) \approx$ ≈ 0.06, while the Ni ions in Cu(2) sites is $x_2 = x - x_1 \approx$ ≈ 0.14. Accordingly, it is comprehensible why Ni doping makes a and b approach mutually but cannot occur the O–T transition, which does actually at $x = 0.12$–0.15 for Fe, Co, and Al doping in Cu–O chains [11,13]. In fact, the O–T transition originates from the stronger cluster effect; for example, the Co E_{mean} is bigger, therefore the oxygen content rises faster with x increasing [16]. Besides, the impure phases appear at $x = 0.25$ for Co doping in Cu–O chains. Correspondingly, the part of Ni ions in Cu–O chains, $x_1 \approx 0.06$, may not induce the impure phases appear. Thus it should be the other part on CuO_2 planes that induce the impure phases appear when $x_2 \approx 0.14$. Similarly, Ref. 13 shows the impure phases appear at $x = 0.12$ for Zn doping. Such results are exhibited gratifyingly from the simulations. In particular, the E_{mean} on CuO_2 planes is less than that in Cu–O chains; therefore the lattice structure of CuO_2 planes is easily destroyed by doped ions. As a result, the impure phases appear in the smaller x. In summary, the cluster effect on CuO_2 planes should be weaker than that in Cu–O chains, where the cluster effect of Ni ions is even weaker than Co, as shown in Tables 2 and 3.

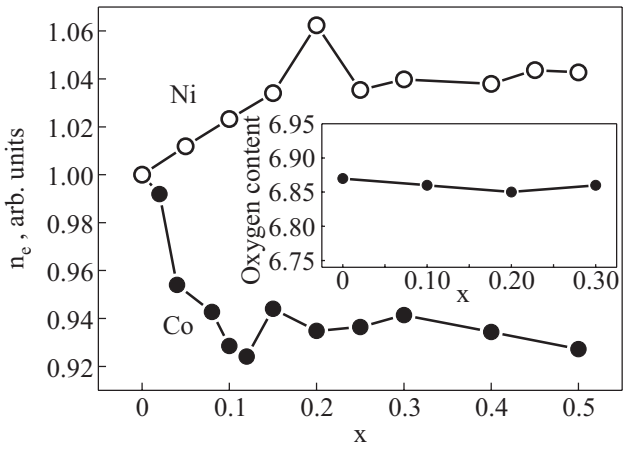

Fig. 3. The variation of reduced local electron density n_e with Ni- and Co-doped concentration x. The inset picture (Ref. 16) indicates the oxygen content variation with x in $YBa_2Cu_{3-x}Ni_xO_{7-\delta}$.

3.3. Ionic cluster effect from PAT experiments

According to the model of two-state captures in condensed matters [20], the process of positron annihilation is attributed to free-state and trapping-state, which correspond to the short lifetime τ_1 and long lifetime τ_2, respectively. The intensity of τ_1 event is I_1, $I_2 = 1 - I_1$ is the intensity of τ_2 event. The short lifetime τ_1 of Ni samples is about 183–200 ps and the long lifetime τ_2 is 450–550 ps around, while the τ_1 intensity I_1 is 85.3–93.0%, other experiments have similar results [21]. For the Co-doped samples, the τ_1 is about 187–203 ps, the τ_2 is about 485–540 ps, while I_1 is about 84.98–87.35%. Positron annihilation rate is $\lambda = \pi r_0^2 c n_e = 1/\tau_{bulk}$, where r_0 is the classical electron radius, c is the speed of light, n_e is local electron density, and τ_{bulk} is the systematical lifetime parameter, which is defined as

$$1/\tau_{bulk} = I_1/\tau_1 + I_2/\tau_2. \qquad (3)$$

The n_e of Ni- and Co-doped samples exhibit opposite trends with x increasing in Fig. 3. The former rises and reaches maximum at $x = 0.20$, then keeps a high saturation. In comparison, the latter drops at relative rapid pace, and reaches minimum at $x = 0.12$, and then presents a low saturation. Some related calculations show that about 90% positrons annihilate with the valence electrons, with only about 10% positrons annihilate with electrons in the atomic kernel, therefore the n_e is determined mainly by the valence electrons [22,23]. While substituting for $Cu^{2.25+}$, +2 valence doped ions make the valence electrons increase in lattices, therefore the n_e rises. In contrast, while substituting for Cu^{2+} in Cu–O chains, +3 valence ions causes the n_e to drop. However, these results cannot explain why both n_e show the saturation feature.

In fact, +3 valence ions tend to enter Cu–O chains. Specifically, a single Co^{3+} ion is less one valence electron than a Cu^{2+}, but it cannot capture one O^{2-} according to the charge equilibrium, therefore the n_e drops. With x increasing, ions form clusters; every two Co^{3+} ions can just capture one O^{2-}, which will attract two valence electrons, consequently the n_e rises. As the n_e dropping and rising reach a balance, the low saturation emerges. With regard to Ni-doped samples, the n_e from Ni^{3+} doping should be of similar pattern to Co^{3+}, namely, it may drop and present a low saturation. On the contrary, while entering CuO_2 planes, a Ni^{2+} has more valence electrons than a $Cu^{2.25+}$ in average, as a result, the n_e should rise. With clusters forming, every four Ni^{2+} may exclude an oxygen ion from CuO_2 planes as stated above, one O^{2-} will take away two valence electrons, thus the n_e will drop. When the n_e rising and dropping achieve a balance, the high saturation emerges. Actually, Ni ions present Ni^{2+} and Ni^{3+} in compounds, and the former amount is 2.33 times of the latter; hence the slow rise of the n_e should exhibit the synthetical results from Ni^{2+} and Ni^{3+}. In a word, the cluster effect induces the n_e to emerge the saturation. What's more, the earlier n_e saturation emerges, the stronger the cluster effect is.

3.4. Ionic cluster effect in suppression on superconductivity

As the above statements, the doped sites are most important factors of influence on the superconductivity. In particular, little doped Ni ions only enter CuO_2 planes, so the T_c is depressed very strongly. If Ni ions continuously enter CuO_2 planes, the T_c should be depressed always very strongly. Actually, a part of Ni ions enter Cu–O chains with x increasing, and then the T_c should be depressed weaker. However, even if the part of Ni ions in Cu–O chains depresses weakly the T_c, the decrease of the T_c should not be slower than that of Co doping in Cu–O chains. Nonetheless, if we only consider the factors of two doped sites, it is hard to explain the cross of the two T_c curves in Fig. 2. In fact, the cluster effect also depresses the T_c. Based on the above analysis, the calculated results and oxygen contents, together with the impure phases and the n_e, show that Ni ions have weaker cluster effect than Co ions in Cu–O chains. Especially on CuO_2 planes, Ni ions exhibit much weaker cluster effect. Furthermore, as transferring from CuO_2 planes to Cu–O chains with x increasing, Ni ions are less and less on CuO_2 planes [21]. Such two causes, the cluster effect and the transformation of Ni ions, make the T_c decrease slower and slower until the cross point in Fig. 2. While the cluster effect is stronger in the Co-doped samples, the superconductivity is suppressed more significantly with x increasing. Therefore, the T_c decrease faster until the cross point before $x = 0.20$. In addition, the previous research results reveal that the magnetism of doped ions has no direct correlation with the superconductivity suppressed in cuprates [11]. Consequently, the magnetism cannot induce two T_c curves to cross each other. In conclusion, excepting the factors of doped sites, the cluster effect is indeed an important factor in suppression of the superconductivity.

4. Conclusions

In the paper, we have conducted systematic research on the high-T_c superconductors $YBa_2Cu_{3-x}(Fe, Ni)_xO_{7-\delta}$ (x = 0–0.5) by means of positron annihilation technique, x-ray diffraction and simulations. The simulated results suggest that ions distribute in dispersive form in little doped concentration. As the doped concentration increases, ions form clusters in the crystal lattice. Ions in Cu–O chains tend to form the cluster of 6 ions, while ions on CuO_2 planes tend to form the cluster of 7 ions. From the simulations and oxygen contents, together with the impure phases and the n_e, we derive the conclusion that the cluster effect not only causes the local electron density to reach the saturation, but also suppresses the superconductivity significantly.

This work is supported by The Natural Science Foundation of China (No. 10647145) and The Natural Science Foundation of Henan Province and Henan Educational Bureau.

1. D.K. Morr and A.V. Balatsky, *Phys. Rev. Lett.* **90**, 067005 (2003).
2. S.Q. Guo, F.L. Wang, Y.L. Zhou, B.R. Zhao, and J. Gao, *Chin. Phys.* **11**, 379 (2002).
3. R. Lortz, C. Meingast, and A.I. Rykov, *Phys. Rev. Lett.* **91**, 20700 (2003).
4. D. de Fontaine, V. Ozolins, Z. Islam, and S.C. Moss, *Phys. Rev.* **B71**, 212504 (2005).
5. Y.S. Lee, Z.Q. Li, W.J. Padilla, S.V. Dordevic, C.C. Homes, Kouji Segawa, Yoichi Ando, and D.N. Basov, *Phys. Rev.* **B72**, 172511 (2005).
6. L.W. Zhang and T.G. Chen, *Acta Physica Sinica* 47, 1906 (1998).
7. J.C. Zhang, L.H. Liu, C. Dong, J.Q. Li, H. Chen, X.G. Li, and G.S. Cheng, *Phys. Rev.* **B65**, 054513 (2002).
8. J.C. Zhang, F.Q. Liu, G.S. Cheng, J.X. Shang, J.Z. Liu, S.X. Cao, and Z.X. Liu, *Phys. Lett.* **A201**, 70 (1995).
9. D.M. Ginsberg, *Physical Properties of High Temperature Superconductors,* World Scientific, Singapore, 538 (1990).
10. Y.K. Kuo, C.W. Schneider, M.J. Skove, M.V. Nevitt, G.X. Tessema, and J.J. McGee, *Phys. Rev.* **B56**, 6201 (1997).
11. P.L. Li, J.C. Zhang, G.X. Cao, D.M. Deng, L.H. Liu, C. Dong, C. Jing, and S.X. Cao, *Acta Physica Sinica* **25**, 1223 (2004).
12. M.S. Islam and C. Ananthamohan, *Phys. Rev.* **B44**, 9492 (1991).
13. P.L. Li, J.C. Zhang, G.X. Cao, C. Jing, and S.X. Cao, *Phys. Rev.* **B69**, 224517 (2004).

14. R.P. Gupta and M. Gupta, *Physica* **C305**, 179 (1998).
15. P.C. Li, H.S. Yang, Z.Q. Li, Y.S. Chai, and L.Z. Cao, *Chin. Phys.* **11**, 285 (2002).
16. J.M. Tarascon, P. Barboux, P.F. Miceli, L.H. Greene, G.W. Hull, M. Eibschutz, and S.A. Sunshine, *Phys. Rev.* **B37**, 7458 (1988).
17. J.M. Tarascon, L.H. Greene, P. Barboux, W.R. McKinnon, G.W. Hull, T.P. Orlando, K.A. Delin, S. Foner, and E.J. McNiff, Jr., *Phys. Rev.* **B36**, 8393 (1987).
18. A.H. MacDonald, *Nature* **414**, 409 (2001).
19. M. Capone, M. Fabrizio, C. Castellani, and E.Tosatti, *Science* **296**, 2364 (2002).
20. W. Brandt, *Positron-Annihilation,* Academic Press, New York (1967).
21. B. Chakraborty, *Phys. Rev.* **B39**, 215 (1989).
22. J.D. Jorgensen, *Phys. Today* **44**, 34 (1991).
23. Y.C. Jean, C.S. Sunder, A. Bharathi, J. Kyle, H. Nakanishi, P.K. Tseng, P.H. Hor, R.L. Meng, Z.J. Huang, C.W. Chu, Z.Z. Wang, P.E.A. Turchi, R.H. Howell, A.L. Wachs, and M.J. Fluss, *Phys. Rev. Lett.* **64**, 1593 (1990).